



# Comparative study between the standard *type I* and the *type A* femtosecond laser induced refractive index change in silver containing glasses

ALAIN ABOU KHALIL,<sup>1,2</sup> JEAN-PHILIPPE BÉRUBÉ,<sup>2</sup> SYLVAIN DANTO,<sup>3</sup> THIERRY CARDINAL,<sup>3</sup> YANNICK PETIT,<sup>1,3</sup> LIONEL CANIONI,<sup>1,\*</sup> AND RÉAL VALLÉE<sup>2</sup>

<sup>1</sup>Université de Bordeaux, CNRS, CEA, CELIA, UMR 5107, F-33405 Talence, France

<sup>2</sup>Centre d'optique, Photonique et Laser (COPL), 2375 Rue de la Terrasse, Université Laval, Québec G1V A06, Canada

<sup>3</sup>Université de Bordeaux, CNRS, ICMCB, UPR 9048, F-33608 Pessac, France

\*lionel.canioni@u-bordeaux.fr

**Abstract:** The femtosecond direct laser writing technique in glasses has been widely used and extensively studied during the last two decades. This technique provides a robust and efficient way to directly inscribe embedded 3D photonic devices in bulk glasses. Following direct laser writing, a local refractive index change ( $\Delta n$ ) is induced that is generally classified under three distinguished types (*type I*, *type II* & *type III*). Each type allows for the fabrication of its own variety of 3D photonic components. However, in silver containing glasses, direct laser writing induces the creation of a new type of refractive index change, called *type Argentum* (*type A*). It is based on the creation of silver clusters that allow for the creation of optical waveguides. In this paper, we report that both *type I* and *type Argentum* modifications could be triggered in silver containing glasses by finely choosing the inscription parameters. A comparative study between both types of single mode waveguides is presented taking into account the morphology,  $\Delta n$  profile and the guided mode profile. Finally, we highlight the originality of *type Argentum* waveguides paving the way for promising applications not accessible by *type I* waveguides.

© 2019 Optical Society of America under the terms of the [OSA Open Access Publishing Agreement](#)

## 1. Introduction

Femtosecond Direct Laser Writing technique (DLW) [1] has been used during the past two decades to create three dimensional (3D) embedded optical components inside glasses for different applications. It consists on focusing a femtosecond laser beam inside transparent materials which induces a permanent refractive index change ( $\Delta n$ ) inside the glass that can be used to form the basis of photonic components. The  $\Delta n$  induced by femtosecond pulses is generally classified as three different types based mainly on the laser fluence: *type I*, *type II* & *type III* [2]. For a given optical material, the three types are generally accessible by adjusting the writing parameters. *Type I* is a smooth refractive index change that can be caused by: a variation of the glass density [3–5] which is due to the local heating and melting followed by a cooling process after laser passage [6], the formation of color centers [4,7,8], or ion exchange in glasses [9]. It consists of an intrinsic modification of the glass matrix itself leading to a  $\Delta n$ . *Type I* refractive index change/modification is the most commonly used for the creation of optical components such as waveguides [10–17], integrated optical components [18–21] and recently quantum photonic circuits in glasses [22,23]. However, it has been reported that *type I* modification could exhibit a negative  $\Delta n$  in some glasses such as BK7 borosilicate [24,25], ZBLAN [26] and phosphate glasses [8,27]. In addition, it was found that the sign of  $\Delta n$  could highly depend on the laser parameters

used as well as the glass composition as reported by several research groups [16,25,26,28], which complicates the creation of *type I* optical waveguides in some glass materials.

Recently, we developed new glasses in which silver ions were incorporated inside the glass matrix as a photosensitive support for DLW [29–31]. In such silver containing glasses, DLW allows the formation of fluorescent silver clusters  $\text{Ag}_m^{x+}$  in the vicinity of the laser-glass interaction voxel [30–33]. Those silver clusters are at the origin of a novel type of refractive index change/modification that we call *type Argentum*, referred to as *type A* for easier reading (based on the Latin name of silver, *Argentum*), acting as an extrinsic modification from the glass matrix itself in silver containing glasses [34]. It allows the creation of optical waveguides as well as photonic components as was demonstrated previously [34].

In this paper, a comparative study between the *type I* and the *type A* refractive index change is presented. We demonstrate that in the same glass substrate made of silver containing zinc phosphate (see Experimental method section for composition and fabrication protocol), *type I* and *type A* refractive index changes could both be induced by wisely adjusting the laser writing parameters. We perform the inscription of single mode waveguides of both types. Then, we present a morphology comparison between both types of waveguides, writing regimes, the  $\Delta n$  profile as well as near field mode profiles. Finally, the advantages of the *type A* modifications are highlighted.

## 2. Experimental method

### 2.1. Glass synthesis

The silver containing zinc phosphate glass investigated in the manuscript have the following composition: 51.3  $\text{PO}_{5/2}$  - 35.2 ZnO - 5.5  $\text{GaO}_{3/2}$ -8  $\text{AgO}_{1/2}$  (mol %). The glass composition corresponds to a pyrophosphate glass composition. Such zinc phosphate glass matrix has been investigated by *Fletcher et al.* in which they noticed a low color center formation [35]. Pyrophosphate are also reported for exhibiting an intermediate photosensitivity towards femtosecond laser irradiation, the metaphosphate having the lowest [36]. The glass was melted using the standard melt-quench technique. High-purity precursors ( $\text{ZnO}$ ,  $\text{Zn}(\text{PO}_3)_2$ ,  $\text{Ga}_2\text{O}_3$ ,  $\text{NaPO}_3$ ,  $\text{AgNO}_3$ ) were weighted in powder forms and mixed together in a platinum crucible. The mix was ramped up ( $1\text{ }^\circ\text{C}\cdot\text{min}^{-1}$ ) at  $1150\text{ }^\circ\text{C}$  and kept at this temperature for 12 hours to assure complete homogenization of the melt. Following the liquid was rapidly quenched in a glassy state and annealed at  $T_g-40\text{ }^\circ\text{C}$  ( $T_g = 380\text{ }^\circ\text{C}$ ) for 4 hours to relax mechanical stress before being slowly cooled down at room temperature. The glass sample was cut and polished to optical quality for the laser inscription process. For the laser injection and the waveguiding characterizing the sample was cut and polished again for a perfect injection and visualization of the guided mode.

### 2.2. Direct laser writing

Two laser setups were used for the inscription of each type of modification. For *type I* waveguides, a chirped pulse amplification system (Coherent RegA) was used, operating at a repetition rate of 250 kHz and emitting at 800 nm with a 100 fs pulse duration. A microscope objective of 50 x - 0.5 NA Nikon was used for the laser inscription. The energy pulses varied from 0.5  $\mu\text{J}$  to 2.5  $\mu\text{J}$ . A quarter-wave plate was inserted in the beam path and adjusted to obtain circularly polarized light. A cylindrical lens telescope (ellipticity of  $a/b = 1/8$ ) was used for beam shaping in order to have circular waveguides. The glass sample was mounted on a mechanical stage (Newport XML210 and GTS30 V). The laser writing occurred 160  $\mu\text{m}$  below the surface using energy pulses going from 0.5  $\mu\text{J}$  to 1  $\mu\text{J}$  and writing speeds of 1 mm/s, 5 mm/s, 10 mm/s and 25 mm/s.

For the inscription of *type A* waveguides, a Yb:KGW femtosecond oscillator (T-pulse 200 by Amplitude systems) was used operating at 9.8 MHz, emitting at 1030 nm wavelength with a pulse duration of 390 fs with an average output power of 2.5 W. The laser irradiance deposited in the

glass was controlled using an acousto-optic modulator enabling the accumulation of  $N = 10^5$ - $10^6$  pulses with energies between 20 nJ and 120 nJ. A 20x - 0.75 NA Zeiss objective was used to focus the laser inside the glass sample which is placed on a high precision 3D stages (XMS-50, Micro controller, Newport). The waveguide was written 160  $\mu\text{m}$  below the surface using a laser irradiance of 9  $\text{TW}/\text{cm}^2$  ( $E_p = 42$  nJ) and a writing speed of 60  $\mu\text{m}/\text{s}$ . Both laser parameters are shown in Table 1. In this paper, the blue color is used to refer to *type I* modification using the Ti:Sapphire laser while the orange color refers to the *type A* modification using the T-pulse 200 laser.

**Table 1. Table summarizing the parameters of the two lasers used for laser writing**

| Laser       | Pulse energy            | Fluence                          | Irradiance                         | Writing speed                   | Microscope objective |
|-------------|-------------------------|----------------------------------|------------------------------------|---------------------------------|----------------------|
| Ti:Sapphire | 0.5 - 2.5 $\mu\text{J}$ | 31 - 56 $\text{J}/\text{cm}^2$   | 680 - 1050 $\text{TW}/\text{cm}^2$ | 1-10 mm/s                       | 50x - 0.5 NA         |
| T-pulse 200 | 20 - 80 nJ              | 0.9 - 2.7 $\text{J}/\text{cm}^2$ | 3 -12 $\text{TW}/\text{cm}^2$      | 10 - 100 $\mu\text{m}/\text{s}$ | 20x - 0.75 NA        |

### 2.3. Mode profile setup

The photo-inscribed waveguides were tested by injecting a 630 nm laser diode using butt-coupling method with an HP-460 fiber (core diameter 2.5  $\mu\text{m}$  – NA = 0.13). Then, a 100x - 0.55 NA Mitutoyo objective was used to collect the near-field guided mode and conjugates it on a high definition CCD camera.

### 2.4. $\Delta n$ measurement

The refractive index change ( $\Delta n$ ) profile and amplitude of all the written waveguides were measured using the SID4Bio wave front sensor by PHASICS Inc under white light illumination. A 50x - 0.55 NA objective was used to visualize the  $\Delta n$  of *type I* waveguides where a 100x-1.3 NA oil immersion objective was used for *type A* waveguides.

## 3. Results and discussion

### 3.1. Morphology comparison

Using two different laser setups both *type I* and *type A* waveguides were inscribed in the same glass substrate. First, we start by characterizing the *type I* waveguides. Series of *type I* waveguides were written typically 160  $\mu\text{m}$  below the glass surface of a silver containing zinc phosphate glass (see Experimental method section) while changing the laser parameters. The pulse energy was varied from 0.5  $\mu\text{J}$  to 1  $\mu\text{J}$  while the writing speed between 1 mm/s and 25 mm/s. For the sake of brevity, only one single mode (SM) *type I* waveguide is fully characterized and compared to a SM *type A* waveguide. *Type I* SM waveguide is obtained using a pulse energy of 0.65  $\mu\text{J}$  and a writing speed of 5 mm/s. Under white light (WL) illumination, the top view of *type I* SM waveguide reveals a single smooth line of modification that is typical of *type I* modification (Fig. 1(a.i)). From the side view, a white colored triangular shape waveguide was observed that is surrounded by a dark ring as shown in Fig. 1(a.iii). Such waveguide morphology was also observed by other research groups in Eagle 200 glasses [37–39]. Under blue excitation, a very weak-fluorescence (compared to *type A* structures) was observed to surround the waveguide under high camera exposure time (Figs. 1(a.ii) - (1.iv)). The weak fluorescence indicates the formation of only few silver clusters following laser inscription. Knowing that the laser writing process is performed using a relatively low repetition laser (250 kHz compared to 9.8 MHz the laser used to create *type A* waveguides) and high writing speeds, the ideal conditions for the creation and aggregation of silver clusters  $\text{Ag}_m^{x+}$  were not met.

On the other hand, direct laser writing process of *type A* waveguides and the optimization of the laser parameters for SM waveguides were reported previously [34]. Herein, we limit

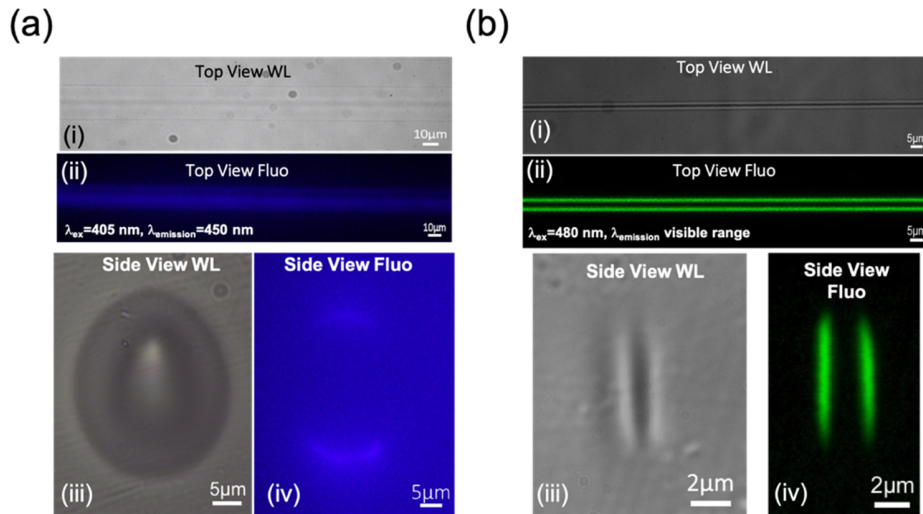


**Fig. 1.** Top View white light illumination (a.i) for *type I* waveguide (b.i) *type A* waveguide. Top view fluorescence of (a.ii) *type I* waveguide (b.ii) *type A* waveguide. Side view white light illumination of (a.iii) *type I* waveguide (b.iii) *type A* waveguide. Side view fluorescence image of (a.iv) *type I* waveguide (b.iv) *type A* waveguide. Two different morphologies were observed for each *type* of modification. The difference of the color of fluorescence is due to different high pass filters used in each observation.

the results to only one SM *type A* waveguide written using a pulse energy of 42 nJ (laser irradiance of 9 TW/cm<sup>2</sup>) and a writing speed of 60 μm/s. The waveguide exhibited a significant fluorescent response under blue excitation (Figs. 1(b.ii) - 1(b.iv)) which is related to the emission of the photo-induced silver clusters as previously reported [30–32,40,41]. Figure 1 shows a morphology comparison between *type I* waveguide and *type A* waveguide under WL illumination and blue excitation. A large heat affected zone is observed for the *type I* waveguides (Fig. 1(a.iii)) compared to a non-existing one for *type A* modification. This indicates that *type I* modification is induced by a thermal inscription regime knowing that the modified zone is larger than the laser focal spot size. The dimensions of the *type I* modified region is 24 μm x 38 μm compared to 3 μm x 6 μm for a *type A* modification (Fig. 1). However, *type I* waveguide exhibited a circular shape which is due to the beam shaping used (see Experimental method section) compared to an elliptical *type A* waveguide where no beam shaping was applied (Fig. 1(a.iii) - 1(b.iii)). Fluorescent confocal images and WL illumination from the top and side view of *type A*, reveal a double line feature following one laser passage (Fig. 1(b)) which is typical of *type A* modification as has been reported before [32,34]. The absence of the fluorescence in the center is due to the photo-dissociation of the silver clusters by the high laser intensity [30–33].

Two different lasers were used for the creation of two different types of modifications. *Type I* modification was induced using a relatively low repetition rate laser of 250 kHz and pulse energies in the order of μJ (0.5 μJ – 1 μJ) and the photo-induced structures were based on a thermal regime due to thermal affected zone observed (Fig. 1(a.iii)). On the other hand, *type A* modification was induced using high repetition rate laser of 9.8 MHz and pulse energies in the order of nJ (20 nJ - 80 nJ) and the photo induced structures were based on an athermal regime (no thermal affected zone) (Fig. 1(b)). It is well known that the thermal inscription regime is directly linked to a high repetition rate laser [42]. Yet, our results reveal a paradoxical phenomenon. In order to understand and explain the results, both laser parameters (fluence and irradiance) as well as the laser absorbed dose as a function of the different writing speeds were calculated (see Appendix

section) and represented as shown in Fig. 2. One can see that the *type A* modification is induced using significantly lower laser fluence in the range of  $0.9 \text{ J/cm}^2$  to  $2.7 \text{ J/cm}^2$  compared to  $31 \text{ J/cm}^2$  to  $56 \text{ J/cm}^2$  for *type I* modification (Fig. 2(a)). Also, a significantly lower laser irradiance for *type A* modification in the range of  $3 \text{ TW/cm}^2$  to  $12 \text{ TW/cm}^2$  compared to higher irradiances of  $680 \text{ TW/cm}^2$  to  $1050 \text{ TW/cm}^2$  for *type I* modification (Fig. 2(b)). In addition to that, a lower laser absorbed dose (ten times less calculated based on the four-photon absorption coefficient [41]) ranging from  $0.04 \text{ J/cm}^3$  to  $2.8 \text{ J/cm}^3$  for *type A* compared to higher values of  $37 \text{ J/cm}^3$  to  $1200 \text{ J/cm}^3$  for *type I* modification as a function of the different writing speeds (Fig. 2(c)). Each regime is induced based on totally different laser parameters and significantly different ranges of laser fluence, irradiance and dose absorbed. Therefore, one can say that the thermal and athermal inscription regimes are not only linked to the laser repetition rate. The laser repetition rate, the energy pulse as well as the writing speed (laser dose deposited) defines the inscription regime whereas it is thermal or athermal. Furthermore, calculating the highest temperature difference  $\Delta T$  that occurs in one point induced by one laser pulse for both lasers confirms our claim (see Appendix section). For the *type A* modification, a maximum  $\Delta T$  of  $10 \text{ K}$  (athermal regime) was calculated compared to a significantly larger value of  $\Delta T$  in the case of *type I* modification. It represents a remarkable increase in the temperature following one laser pulse that can heat the glass above the transition temperature  $T_g$  and melts it resulting in a thermal inscription regime.

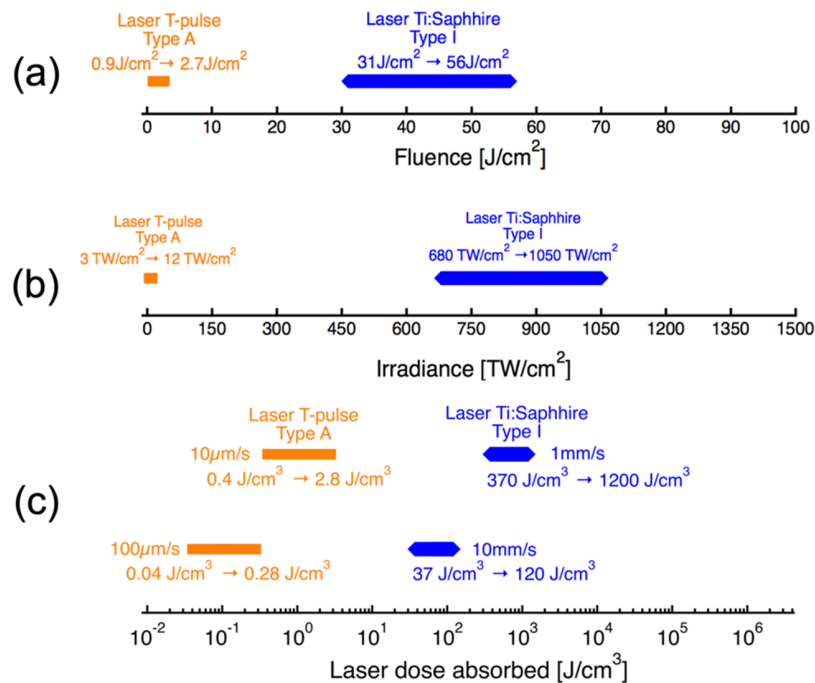


**Fig. 2.** Laser parameters for both lasers used for the writing process: (orange) T-pulse 200 laser used for the inscription of *type A* modification, (blue) Ti:Sapphire laser used for the inscription of *type I* modification. (a) laser fluence (b) laser irradiance (c) calculated laser dose absorbed as a function of the writing speed.

### 3.2. Refractive index and mode profiles

The refractive index change ( $\Delta n$ ) for the *type I* SM waveguide was measured using the Quadri-Wave Lateral Shearing Interferometry (QWLSI) (see Experimental method section) as shown in Fig. 3. A smooth line of refractive index change was observed from the top view which is

typical of *type I* modification (Fig. 3(a.i)). The  $\Delta n$  profile extracted from the phase image reveal a positive  $\Delta n$  peak surrounded by a negative  $\Delta n$  (Fig. 3(a.ii)). Going back to the side view image of the waveguide under WL illumination (Fig. 1(a.iii)), one can correlate the bright part to a positive  $\Delta n$  and the dark ring to a negative  $\Delta n$  acting as a depressed cladding. The positive  $\Delta n$  peak was measured to be  $\sim 2 \times 10^{-3}$  as shown in (Fig. 3(a.ii)). Compared to the pristine glass's refractive index, the positive peak exists well below it. The laser inscription process induces a strong negative  $\Delta n$  on the edges but a positive  $\Delta n$  peak in the center (Fig. 3(a.ii)). Whereas, for the *type A* modification shown in (Fig. 3(b)), a positive double line feature is observed from the top view phase imaging which is expected [34]. The  $\Delta n$  profile consists of two positive  $\Delta n$  peaks of  $2.3 \times 10^{-3}$  each, spatially associated to the silver cluster distributions as previously reported [34]. Therefore, each type of modification exhibits totally different  $\Delta n$  profiles.

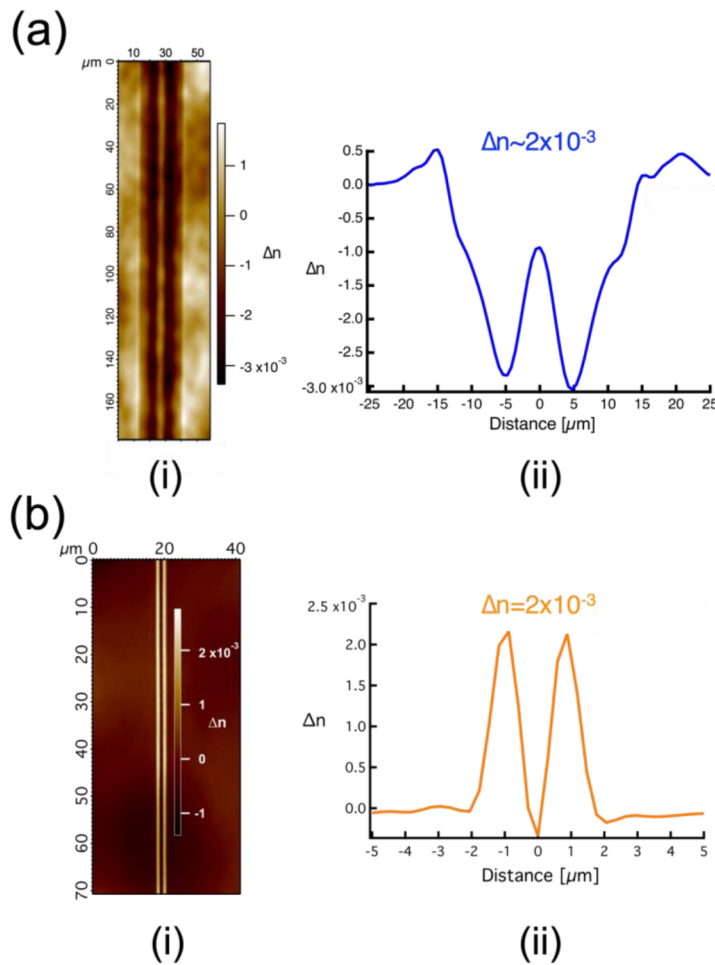


**Fig. 3.** Top view phase image of (a.i) *type I* waveguide, (b.i) *type A* waveguide. Refractive index profile of (a.ii) *type I* waveguide exhibiting one single positive  $\Delta n$  peak of  $2 \times 10^{-3}$ , (b.ii) *type A* waveguide exhibiting two positive  $\Delta n$  peaks of  $2.3 \times 10^{-3}$ . DLW conditions for *type I*: ( $E_p = 0.65 \mu\text{J}$  -  $v = 5 \text{ mm/s}$  -  $T_{\text{rep}} = 250 \text{ kHz}$  -  $\text{NA} = 0.55$  -  $160 \mu\text{m}$  below the surface), *type A* ( $E_p = 42 \text{ nJ}$  -  $v = 60 \mu\text{m/s}$  -  $T_{\text{rep}} = 9.8 \text{ MHz}$  -  $\text{NA} = 0.75$  -  $160 \mu\text{m}$  below the surface).

Following  $\Delta n$  characterization, the sample was installed on the transmission setup and a 630 nm diode laser was injected inside the waveguides (see Experimental method section). The near-field mode profile following laser injection in each type of waveguides is shown in Fig. 4. For the SM *type I* waveguide, a circular mode profile was observed that is the fundamental mode LP<sub>01</sub>. Horizontal and vertical line profiles show that the mode is a Gaussian one of  $4.5 \mu\text{m} \times 5.2 \mu\text{m}$ , almost a circular one. Even though the waveguide exhibited large dimensions of  $24 \mu\text{m} \times 38 \mu\text{m}$ , the guiding region is only around  $5 \mu\text{m} \times 5 \mu\text{m}$  which is correlated to the white region under white illumination (Fig. 1(a.iii)) exhibiting a positive  $\Delta n$  peak (Fig. 3(a.ii)). The large dimensions of the modified zone are due to the heat affected zone that is generated following laser inscription. For the *type A* SM waveguide, the fundamental mode is an elliptical mode supported by two close and highly interacting waveguides [34]. One should recall that for the inscription of *type I* waveguides, the beam was shaped in order to have circular waveguides which was not the case for the inscription of *type A* waveguides. Even though the *type I* waveguide exhibited larger dimensions compared to *type A*, the guided mode profile's dimensions are comparable,  $4.5 \mu\text{m} \times 5.2 \mu\text{m}$  compared to  $3 \mu\text{m} \times 5.2 \mu\text{m}$  respectively. The propagation losses of the *type I* waveguide in this case were estimated to exhibit upper value of 4.5 dB/cm (estimated using the same method as in [34]) which is quite high compared to *type A* waveguide losses of 1.2 dB/cm [34]. The high losses of the *type I* waveguide could be explained by the inhomogeneity of the glass sample as well as the formation of defects during the laser inscription. Moreover, self-periodic ripples were sometimes observed during the writing process which could explain the waveguides' high losses. No further efforts were put to create low losses *type I* waveguide, yet, waveguides exhibiting losses below 0.4 dB/cm were reported by other research groups in phosphate based glasses [13,43].

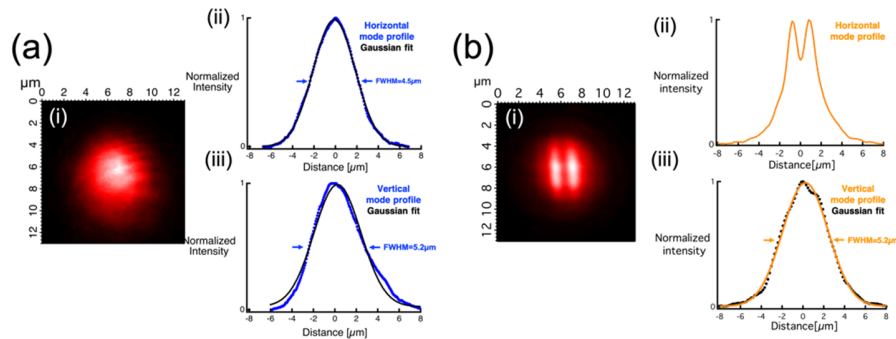


**Fig. 4.** Near-field mode profile following laser injection at 630 nm for (a.i) *type I* waveguide (b.i) *type A* waveguide. Normalized horizontal intensity averaged along the horizontal axis of (a.ii) *type I* mode profile exhibiting a FWHM of  $4.5 \mu\text{m}$  (b.ii) *type A* mode profile. Normalized vertical intensity average along the vertical axis of (a.iii) *type I* mode profile exhibiting a FWHM of  $5.2 \mu\text{m}$  (b.iii) *type A* mode profile exhibiting a FWHM of  $5.2 \mu\text{m}$ . A circular mode profile exhibited by *type I* waveguide compared to an elliptical one for *type A* waveguide while exhibiting more or less the same dimensions.

### 3.3. Flipping $\Delta n$ and *type A* advantages

The refractive index change ( $\Delta n$ ) of all the written *type I* structures/waveguides was measured. It was found that the *type I*  $\Delta n$  is flipping its sign as a function of the laser parameters (Fig. 5(a)) which was also reported before by many research groups [8,25–27]. Using a higher writing speed (Fig. 5(a.I)) or lower pulse energy (Fig. 5(a.ii)) induces the flipping of the  $\Delta n$  from positive to negative. Indeed, one can observe that the initial material response following laser inscription tends to be a negative  $\Delta n$ , yet increasing the laser deposited dose (lower speed of writing and/or

higher energy pulse), induces the rising of a positive  $\Delta n$  peak in the middle of the interaction voxel (Fig. 5(a)). Compared to *type A* modification, the photo-induced  $\Delta n$  is always a positive one as shown in Fig. 5(b). No matter what the conditions of DLW were, a positive *type A*  $\Delta n$  is observed as long as they exceed the threshold of creation of silver clusters  $\text{Ag}_m^{x+}$ .

As a closure, one can say that wisely choosing the laser parameters, and the laser regime, either *type I* or *type A* modification could be triggered inside silver containing glasses. *Type I* modification is an intrinsic modification acting on the glass matrix itself where the photo-induced  $\Delta n$ , positive or negative could be generally based on the creation of color centers [4,7,8] and/or a change in the glass density [3–5]. On the other hand, *Type A* modification is an extrinsic modification where the laser energy acts on the photo-chemistry inside the glass matrix by photo-exciting the pre-existing silver ions  $\text{Ag}^+$  and developing the silver clusters  $\text{Ag}_m^{x+}$  responsible for the positive  $\Delta n$  and supporting the waveguiding properties. *Type A* occurs in the low pulse energy regime (20 nJ – 80 nJ) compared to *type I* (0.5  $\mu\text{J}$  – 1  $\mu\text{J}$ ) as shown in Fig. 6. This type of modification presents some advantages compared to the well-known *type I*. It always exhibits a positive  $\Delta n$  following laser inscription, however, the *type I* modification could be a positive or a negative one based on the glass composition [16] or the laser parameters [25,26] which complicates the creation of optical components. *Type A* waveguide exhibited smaller dimensions in this case specifically knowing that in our experiments the *type I* modification exhibited remarkably large dimensions. Finally, one of the most important advantages of *type A* modification is the capability of writing near-surface waveguides (in the low pulse energy regime) with no need for additional processing which is not the case with *type I* modification [44].

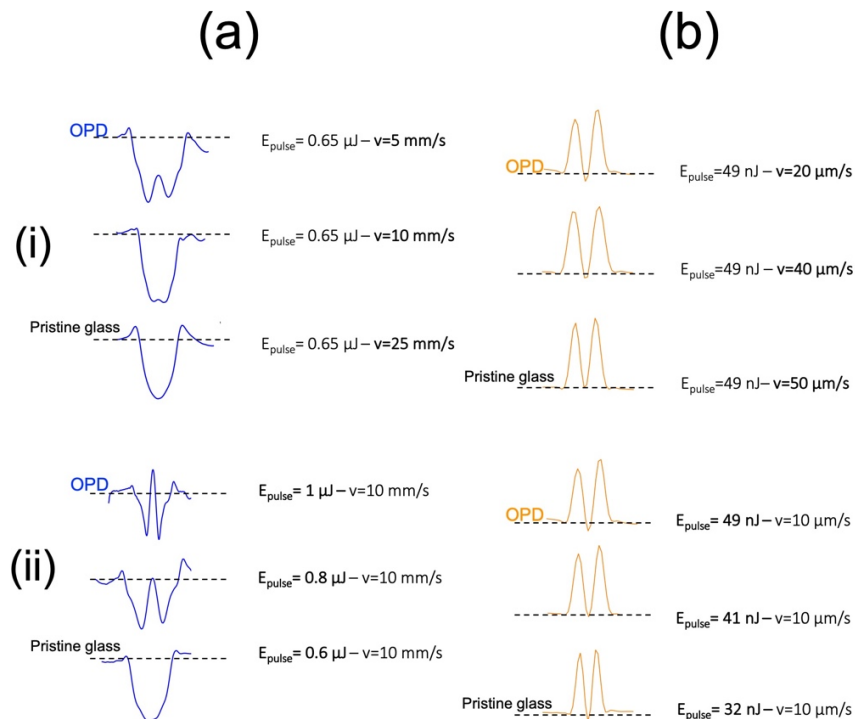


**Fig. 5.** Various optical path differences (OPD) profiles measured by the SID4Bio (see Experimental method section) for (a) *type I* waveguides (b) *type A* waveguides as a function of the (i) writing speed (ii) pulse energy. The *type I*  $\Delta n$  flips its sign as a function of the laser parameters whereas *type A* is always a positive one. The  $\Delta n$  values are retrieved from the OPD measured using the SID4Bio by dividing the OPD by the thickness of the waveguide.

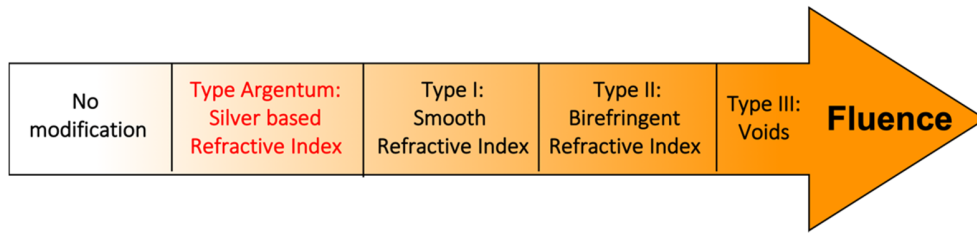


**Fig. 6.** The new suggested classification of the different types of modification/refractive index change fluence in glasses as a function of the laser fluence.

#### 4. Conclusion

In silver containing glasses, wisely choosing the laser parameters, either *type I* or *type A* modifications could be triggered in the same glass substrate. The *type I* modifications are formed using the thermal regime with high laser fluence and a low repetition laser (250 kHz) compared to an athermal regime for *type A* modification using a low laser fluence and a high repetition laser rate (9.8 MHz). Single mode waveguides of each type (*type I* and *type A*) were inscribed in the same glass substrate. A morphology comparison between two single mode waveguides of each type reveals a large heat affected zone for *type I* modification compared to a non-existing one for *type A*. The overall waveguides dimensions are  $24\ \mu\text{m} \times 38\ \mu\text{m}$  and  $3\ \mu\text{m} \times 6\ \mu\text{m}$  respectively for *type I* and *type A* waveguides. However, the guided mode profiles dimensions are roughly identical knowing that the guiding region of *type I* waveguide is  $5\ \mu\text{m} \times 5\ \mu\text{m}$ . Moreover, the  $\Delta n$  of *type I* flips from positive to negative as a function of the laser parameters whereas the *type A* modification is always a positive one. In closing, we report a type of modification called *type A* (referring to the Latin name of silver, *Argentum*), based on the creation of silver clusters  $\text{Ag}_m^{x+}$  that occurs in the low pulse energy regime sitting well below the well-known *type I* modification. This new type exhibits many advantages compared to *type I*: always positive  $\Delta n$ , smaller structures' dimensions and the capability of writing near-surface waveguides paving the way towards interesting sensing and spectroscopy applications.

#### Appendix:

The highest temperature difference  $\Delta T$  that occurs in one point induced by one laser pulse as given by:

$$\Delta T = \frac{Q_0}{\rho C_p} \quad (1)$$

where  $Q_0$  is the energy deposited by voxel,  $\rho$  is the molar density of the glass and  $C_p$  the heat capacity.

The energy deposited by voxel  $Q_0$  is obtained by dividing the energy deposited  $E_D$  by the volume of the voxel:

$$Q_0 = \frac{E_D}{\pi^{3/2} w_{NL}^2 z_{NL}} \quad (2)$$

where the energy deposited  $E_D$  is given by:

$$E_D = \alpha^{(4)} 9T\pi \left(\frac{w_{NL}}{3}\right)^2 I^4 \frac{3}{4} z_{NL} \quad (3)$$

With  $\alpha^{(4)} = 14.6 \pm 1 \times 10^{-3} \text{ cm}^5 / \text{TW}^3$  is the estimated coefficient absorption corresponding to the four photon process (measured using a pump-probe experiment) [41],  $T$  is the laser repetition rate with  $w_{NL} = \frac{w_0}{\sqrt{N}}$  and  $z_{NL} = \frac{z_r}{\sqrt{N}}$  the non-linear waist and Rayleigh length with  $N = 4$  corresponding

to a four photon absorption effect, and  $I$  the laser irradiance. The deposited energy calculated for parameters used for *type I* modification exceeded the energy of the pulse which is not normal. The formula used in that case is not fully compatible when using high pulse energies and three photon absorption. Therefore, the energy deposited was limited to 1  $\mu\text{J}$ . Finally, those calculations are only approximate to show the large difference between the two laser parameters used.

## Funding

Agence Nationale de la Recherche (ANR) (NR-10-IDEX-03-02); H2020 Marie Skłodowska-Curie Actions (MSCA) (No 823941.); Natural Sciences and Engineering Research Council of Canada (NSERC) (CG101779); Canada Foundation for Innovation (CFI) (GF072345); Fonds de Recherche du Québec - Nature et Technologies (FRQNT) (CO201310, FT097991).

## Acknowledgments

This research was funded by French National Research Agency (ANR), in the framework of the “Investments for the Future” program, with the reference number LAPHIA ANR - n °ANR-10-IDEX-03-02 and Natural Sciences and Engineering Research Council of Canada (NSERC) (CG101779), Canada Foundation for Innovation (CFI) (GF072345), and Fonds de Recherche du Québec-Nature et Technologies (FRQNT) (FT097991, CO201310). The project has also received funding from the European Union’s Horizon 2020 research and innovation programme under the Marie Skłodowska-Curie grant agreement No 823941.

The authors would like to thank Stéphane Gagnon for cutting and polishing the glass samples.

## Disclosures

The authors declare that there are no conflicts of interest related to this article.

## References

1. K. M. Davis, K. Miura, N. Sugimoto, and K. Hirao, “Writing waveguides in glass with a femtosecond laser,” *Opt. Lett.* **21**(21), 1729–1731 (1996).
2. B. Poumellec, M. Lancry, A. Chahid-Erraji, and P. Kazansky, “Modification thresholds in femtosecond laser processing of pure silica: review of dependencies on laser parameters [Invited],” *Opt. Mater. Express* **1**(4), 766–782 (2011).
3. J. W. Chan, T. R. Huser, S. H. Risbud, J. S. Hayden, and D. M. Krol, “Waveguide fabrication in phosphate glasses using femtosecond laser pulses,” *Appl. Phys. Lett.* **82**(15), 2371–2373 (2003).
4. J. W. Chan, T. R. Huser, S. H. Risbud, and D. M. Krol, “Modification of the fused silica glass network associated with waveguide fabrication using femtosecond laser pulses,” *Appl. Phys. A: Mater. Sci. Process.* **76**(3), 367–372 (2003).
5. L. B. Fletcher, J. J. Witcher, W. B. Reichman, A. Arai, J. Bovatsek, and D. M. Krol, “Changes to the network structure of Er–Yb doped phosphate glass induced by femtosecond laser pulses,” *J. Appl. Phys.* **106**(8), 083107 (2009).
6. C. B. Schaffer, J. F. García, and E. Mazur, “Bulk heating of transparent materials using a high-repetition-rate femtosecond laser,” *Appl. Phys. A* **76**(3), 351–354 (2003).
7. A. M. Streltsov and N. F. Borrelli, “Study of femtosecond-laser-written waveguides in glasses,” *J. Opt. Soc. Am. B* **19**(10), 2496–2504 (2002).
8. D. J. Little, M. Ams, P. Dekker, G. D. Marshall, and M. J. Withford, “Mechanism of femtosecond-laser induced refractive index change in phosphate glass under a low repetition-rate regime,” *J. Appl. Phys.* **108**(3), 033110 (2010).
9. S. Kanehira, K. Miura, and K. Hirao, “Ion exchange in glass using femtosecond laser irradiation,” *Appl. Phys. Lett.* **93**(2), 023112 (2008).
10. M. Will, S. Nolte, B. N. Chichkov, and A. Tünnermann, “Optical properties of waveguides fabricated in fused silica by femtosecond laser pulses,” *Appl. Opt.* **41**(21), 4360–4364 (2002).
11. R. Osellame, S. Taccheo, M. Marangoni, R. Ramponi, P. Laporta, D. Polli, S. De Silvestri, and G. Cerullo, “Femtosecond writing of active optical waveguides with astigmatically shaped beams,” *J. Opt. Soc. Am. B* **20**(7), 1559–1567 (2003).
12. L. Shah, A. Arai, S. Eaton, and P. Herman, “Waveguide writing in fused silica with a femtosecond fiber laser at 522 nm and 1 MHz repetition rate,” *Opt. Express* **13**(6), 1999–2006 (2005).
13. M. Ams, G. Marshall, D. Spence, and M. Withford, “Slit beam shaping method for femtosecond laser direct-write fabrication of symmetric waveguides in bulk glasses,” *Opt. Express* **13**(15), 5676–5681 (2005).

14. J. P. Berube, S. H. Messaddeq, M. Bernier, I. Skripachev, Y. Messaddeq, and R. Vallee, "Tailoring the refractive index of Ge-S based glass for 3D embedded waveguides operating in the mid-IR region," *Opt. Express* **22**(21), 26103–26116 (2014).
15. J. Lapointe, M. Gagne, M. J. Li, and R. Kashyap, "Making smart phones smarter with photonics," *Opt. Express* **22**(13), 15473–15483 (2014).
16. L. B. Fletcher, J. J. Witcher, N. Troy, S. T. Reis, R. K. Brow, and D. M. Krol, "Direct femtosecond laser waveguide writing inside zinc phosphate glass," *Opt. Express* **19**(9), 7929–7936 (2011).
17. P. S. Salter, A. Jesacher, J. B. Spring, B. J. Metcalf, N. Thomas-Peter, R. D. Simmonds, N. K. Langford, I. A. Walmsley, and M. J. Booth, "Adaptive slit beam shaping for direct laser written waveguides," *Opt. Lett.* **37**(4), 470–472 (2012).
18. W.-J. Chen, S. M. Eaton, H. Zhang, and P. R. Herman, "Broadband directional couplers fabricated in bulk glass with high repetition rate femtosecond laser pulses," *Opt. Express* **16**(15), 11470 (2008).
19. S. Nolte, M. Will, J. Burghoff, and A. Tünnemann, "Femtosecond waveguide writing: a new avenue to three-dimensional integrated optics," *Appl. Phys. A: Mater. Sci. Process.* **77**(1), 109–111 (2003).
20. K. Minoshima, A. M. Kowalevicz, E. P. Ippen, and J. G. Fujimoto, "Fabrication of coupled mode photonic devices in glass by nonlinear femtosecond laser materials processing," *Opt. Express* **10**(15), 645–652 (2002).
21. J. Lapointe, F. Parent, E. S. de Lima Filho, S. Loranger, and R. Kashyap, "Toward the integration of optical sensors in smartphone screens using femtosecond laser writing," *Opt. Lett.* **40**(23), 5654–5657 (2015).
22. G. D. Marshall, A. Politi, J. C. F. Matthews, P. Dekker, M. Ams, M. J. Withford, and J. L. O'Brien, "Laser written waveguide photonic quantum circuits," *Opt. Express* **17**(15), 12546–12554 (2009).
23. F. Flamini, L. Magrini, A. S. Rab, N. Spagnolo, V. D'Ambrosio, P. Mataloni, F. Sciarrino, T. Zandrin, A. Crespi, R. Ramponi, and R. Osellame, "Thermally reconfigurable quantum photonic circuits at telecom wavelength by femtosecond laser micromachining," *Light: Sci. Appl.* **4**(11), e354 (2015).
24. D. J. Little, M. Ams, S. Gross, P. Dekker, C. T. Miese, A. Fuerbach, and M. J. Withford, "Structural changes in BK7 glass upon exposure to femtosecond laser pulses," *J. Raman Spectrosc.* **42**(4), 715–718 (2011).
25. A. Mermillod-Blondin, I. M. Burakov, Y. P. Meshcheryakov, N. M. Bulgakova, E. Audouard, A. Rosenfeld, A. Husakou, I. V. Hertel, and R. Stoian, "Flipping the sign of refractive index changes in ultrafast and temporally shaped laser-irradiated borosilicate crown optical glass at high repetition rates," *Phys. Rev. B* **77**(10), 104205 (2008).
26. J.-P. Bérubé, M. Bernier, and R. Vallée, "Femtosecond laser-induced refractive index modifications in fluoride glass," *Opt. Mater. Express* **3**(5), 598–611 (2013).
27. S. Gross, M. Ams, G. Palmer, C. T. Miese, R. J. Williams, G. D. Marshall, A. Fuerbach, D. G. Lancaster, H. Ebendorff-Heidepriem, and M. J. Withford, "Ultrafast Laser Inscription in Soft Glasses: A Comparative Study of Athermal and Thermal Processing Regimes for Guided Wave Optics," *Int. J. Appl. Glass Sci.* **3**(4), 332–348 (2012).
28. D. Ehrhart, T. Kittel, M. Will, S. Nolte, and A. Tünnemann, "Femtosecond-laser-writing in various glasses," *J. Non-Cryst. Solids* **345-346**, 332–337 (2004).
29. C. Maurel, T. Cardinal, M. Bellec, L. Canioni, B. Bousquet, M. Treguer, J. J. Videau, J. Choi, and M. Richardson, "Luminescence properties of silver zinc phosphate glasses following different irradiations," *J. Lumin.* **129**(12), 1514–1518 (2009).
30. M. Bellec, A. Royon, B. Bousquet, K. Bourhis, M. Treguer, T. Cardinal, M. Richardson, and L. Canioni, "Beat the diffraction limit in 3D direct laser writing in photosensitive glass," *Opt. Express* **17**(12), 10304–10318 (2009).
31. M. Bellec, A. Royon, K. Bourhis, J. Choi, B. Bousquet, M. Treguer, T. Cardinal, J.-J. Videau, M. Richardson, and L. Canioni, "3D Patterning at the Nanoscale of Fluorescent Emitters in Glass," *J. Phys. Chem. C* **114**(37), 15584–15588 (2010).
32. J.-C. Desmoulin, Y. Petit, L. Canioni, M. Dussauze, M. Lahaye, H. M. Gonzalez, E. Brasselet, and T. Cardinal, "Femtosecond laser structuring of silver-containing glass: Silver redistribution, selective etching, and surface topology engineering," *J. Appl. Phys.* **118**(21), 213104 (2015).
33. E. Smetanina, B. Chimier, Y. Petit, N. Varkentina, E. Fargin, L. Hirsch, T. Cardinal, L. Canioni, and G. Duchateau, "Modeling of cluster organization in metal-doped oxide glasses irradiated by a train of femtosecond laser pulses," *Phys. Rev. A* **93**(1), 013846 (2016).
34. A. Abou Khalil, J.-P. Bérubé, S. Danto, J.-C. Desmoulin, T. Cardinal, Y. Petit, R. Vallée, and L. Canioni, "Direct laser writing of a new type of waveguides in silver containing glasses," *Sci. Rep.* **7**(1), 11124 (2017).
35. L. B. Fletcher, J. J. Witcher, N. Troy, S. T. Reis, R. K. Brow, R. M. Vazquez, R. Osellame, and D. M. Krol, "Femtosecond laser writing of waveguides in zinc phosphate glasses [Invited]," *Opt. Mater. Express* **1**(5), 845–855 (2011).
36. T. Guérineau, L. Loi, Y. Petit, S. Danto, A. Fargues, L. Canioni, and T. Cardinal, "Structural influence on the femtosecond laser ability to create fluorescent patterns in silver-containing sodium-gallium phosphate glasses," *Opt. Mater. Express* **8**(12), 3748–3760 (2018).
37. A. Arriola, S. Gross, N. Jovanovic, N. Charles, P. G. Tuthill, S. M. Olaizola, A. Fuerbach, and M. J. Withford, "Low bend loss waveguides enable compact, efficient 3D photonic chips," *Opt. Express* **21**(3), 2978–2986 (2013).
38. S. M. Eaton, H. Zhang, M. L. Ng, J. Li, W.-J. Chen, S. Ho, and P. R. Herman, "Transition from thermal diffusion to heat accumulation in high repetition rate femtosecond laser writing of buried optical waveguides," *Opt. Express* **16**(13), 9443–9458 (2008).

39. N. Jovanovic, S. Gross, C. Miese, A. Fuerbach, J. Lawrence, and M. Withford, "Direct Laser Written Multimode Waveguides for Astronomical Applications," in *Advanced Photonics & Renewable Energy* (Optical Society of America, Karlsruhe, 2010), p. JThA28.
40. Y. Petit, S. Danto, T. Guérineau, A. Abou Khalil, A. Le Camus, E. Fargin, G. Duchateau, J.-P. Bérubé, R. Vallée, Y. Messaddeq, T. Cardinal, and L. Canioni, "On the femtosecond laser-induced photochemistry in silver-containing oxide glasses: mechanisms, related optical and physico-chemical properties, and technological applications," *Adv. Opt. Technol.* **7**(5), 291–309 (2018).
41. K. Bourhis, A. Royon, M. Bellec, J. Choi, A. Fargues, M. Treguer, J.-J. Videau, D. Talaga, M. Richardson, T. Cardinal, and L. Canioni, "Femtosecond laser structuring and optical properties of a silver and zinc phosphate glass," *J. Non-Cryst. Solids* **356**(44-49), 2658–2665 (2010).
42. S. Eaton, H. Zhang, P. Herman, F. Yoshino, L. Shah, J. Bovatsek, and A. Arai, "Heat accumulation effects in femtosecond laser-written waveguides with variable repetition rate," *Opt. Express* **13**(12), 4708–4716 (2005).
43. R. Osellame, G. Della Valle, N. Chiodo, S. Taccheo, P. Laporta, O. Svelto, and G. Cerullo, "Lasing in femtosecond laser written optical waveguides," *Appl. Phys. A* **93**(1), 17–26 (2008).
44. J.-P. Bérubé and R. Vallée, "Femtosecond laser direct inscription of surface skimming waveguides in bulk glass," *Opt. Lett.* **41**(13), 3074–3077 (2016).